

Chemical evolution of the Fornax dwarf spheroidal galaxy

D. Ponce¹, G. A. Lanfranchi¹ & A. Caproni¹

¹ Núcleo de Astrofísica – NAT, Universidade Cidade de São Paulo

Abstract. The Fornax dwarf spheroidal galaxy, a distant Milky Way satellite, contains intermediate-age and old stellar populations with $[\text{Fe}/\text{H}] \approx -1.0$ dex. Its absence of neutral gas suggests loss through internal winds or external processes. This study combines chemical evolution models and 3D hydrodynamical simulations to analyze its gaseous evolution and compare these results with observed abundances and masses. Supernova rates and stellar mass changes guide the simulations, clarifying enrichment and evolution. The results show that both internal and external mechanisms shape Fornax and highlight the need for integrated chemical–dynamical modeling.

Resumo. A galáxia anã esferoidal Fornax, um satélite distante da Via Láctea, apresenta populações estelares intermediárias e antigas, com $[\text{Fe}/\text{H}] \approx -1.0$ dex. A falta de gás neutro indica perda por ventos internos ou processos externos. Este estudo combina modelos de evolução química e simulações hidrodinâmicas 3D para analisar sua evolução gasosa e compará-la às abundâncias e massas observadas. As taxas de supernovas e variações de massa estelar orientam as simulações, esclarecendo o enriquecimento e a evolução. Os resultados mostram que mecanismos internos e externos moldam Fornax e destacam a importância de integrar modelagem química e dinâmica.

Keywords. Galaxies: dwarf – formation – evolution

1. Introduction

Over recent decades, the chemical enrichment of classical dwarf spheroidal galaxies (dSphs) in the Local Group has been widely examined (Shetrone et al. 2001, 2003; Venn et al. 2004; Geisler et al. 2005; Hill, Tolstoy & Tosi 2009; Kirby et al. 2010; Venn et al. 2012; de Boer et al. 2012a, 2012b; Koch et al. 2013), revealing old, metal-poor populations. Their proximity enables detailed abundance studies (Mateo 1998; Kunth & Ostlin 2000). Most dSphs host ancient stars (>10 Gyr; Tolstoy, Hill & Tosi 2009), and relations such as age–metallicity, MDF, and abundance ratios depend on the SFH, IMF, and yields (Matteucci 1996), highlighting the relevance of chemical evolution models.

The Fornax dSph, a distant (~ 135 kpc; Rizzi et al. 2007) and luminous Milky Way satellite with mass $\sim 10^7 M_{\odot}$ (Walker et al. 2007), exhibits a complex SFH with intermediate-age, ancient, and young populations (Dolphin et al. 2005; Battaglia et al. 2006; Coleman & de Jong 2008). Its mean metallicity, $[\text{Fe}/\text{H}] \approx -1.0$ dex (Pont et al. 2004), was reached early, though models do not fully match the observed $[\alpha/\text{Fe}]$ trends (Kirby et al. 2010). Surveys (de Boer et al. 2012a) show dominance of 1–10 Gyr stars. The age–metallicity relation indicates rapid early enrichment, followed by slower growth to $[\text{Fe}/\text{H}] \sim -0.8$ dex. The decline in $[\text{Mg}/\text{Fe}]$ for $[\text{Fe}/\text{H}] \geq -1.5$ dex (Letarte et al. 2010; Kirby et al. 2010) suggests reduced star formation rates compared to the solar neighborhood (Ikuta & Arimoto 2002; Carigi, Hernandez & Gilmore 2002; Lanfranchi & Matteucci 2004), reflecting the complexity of Fornax’s chemical evolution.

2. Methodology

The evolution of the Fornax dwarf spheroidal galaxy will be analyzed by combining chemical evolution models (Lanfranchi & Matteucci 2003, 2004, 2010) with three-dimensional hydrodynamical simulations using the PLUTO code, previously applied to Ursa Minor (Caproni et al. 2015, 2017). This approach is crucial because chemical models lack internal gas dynamics, while simulations provide self-consistent mass-loss rates (Fenner et al. 2006; Hendricks et al. 2014). The model assumes galac-

tic winds proportional to the SFR, activated when gas kinetic energy exceeds the gravitational binding energy, including the dark matter halo (Lanfranchi & Matteucci 2003, 2004), in agreement with previous simulations (Ruiz et al. 2013; Caproni et al. 2015, 2017). Consequently, parameters from the chemical models—such as star formation history, SFR, stellar mass, and supernova rates—will support future hydrodynamical simulations, enabling comparisons between predicted and simulated mass-loss rates and clarifying the influence of galactic winds on Fornax’s evolution.

3. Observational Data

Over the last decades, extensive observations of Fornax—chemical abundances (Letarte et al. 2006, 2010; Battaglia et al. 2006; Kirby et al. 2010), stellar populations, formation history (Dolphin et al. 2005; Battaglia et al. 2006; Coleman & de Jong 2008; de Boer et al. 2012), mass (Walker et al. 2007), and mean metallicity (Pont et al. 2004)—have enabled detailed evolutionary analyses. Abundance ratios were obtained from the globular cluster of Letarte et al. (2006) and giant stars in Letarte et al. (2010), while Battaglia et al. (2006) derived an MDF from the CaT for ~ 560 stars, consistent with previous studies. Star formation histories from color–magnitude diagrams (Saviane et al. 2000; de Boer et al. 2012a; Coleman & de Jong 2008; Letarte et al. 2010) were used as initial conditions. Saviane, Coleman & Letarte propose two long episodes (~ 4 – 5 Gyr) separated by ~ 2 – 3 Gyr and followed by a short recent burst, whereas de Boer et al. (2012a) suggest continuous but variable star formation. Both scenarios indicate a peak at intermediate ages, with episode efficiencies treated as free parameters in this study.

4. Results

The chemical evolution model of Lanfranchi & Matteucci (2003, 2004, 2010) was calibrated for the Fornax dwarf spheroidal galaxy by adjusting the star formation efficiency (η_{SF}), wind

efficiency (w_i), and infall timescale (t_{inf}) using the observational constraints described in the methodology. Three scenarios were tested: Model 1 (solid black) with a single episode and $\eta_{\text{SF}} = 1.03 \text{ Gyr}^{-1}$, $w_i = 5.86$, $t_{\text{inf}} = 1.22 \text{ Gyr}$; Model 2 (blue dashed), also single-episode, with $\eta_{\text{SF}} = 1.01 \text{ Gyr}^{-1}$, $w_i = 5.86$, $t_{\text{inf}} = 0.42 \text{ Gyr}$; and Model 3 (red dash-dot), with three episodes and $\eta_{\text{SF},1} = 1.10 \text{ Gyr}^{-1}$, $\eta_{\text{SF},2} = 0.39 \text{ Gyr}^{-1}$, $\eta_{\text{SF},3} = 0.86 \text{ Gyr}^{-1}$, $w_i = 5.59$, $t_{\text{inf}} = 0.81 \text{ Gyr}$. These models reproduced Fornax's star formation history, the type Ia (binary fraction of 87%) and type II SN rates, the abundances of Ca, Si, O, and Mg, the evolution of total, stellar, and gas masses, the age–metallicity relation, and the MDF for the three scenarios (black, blue, red).

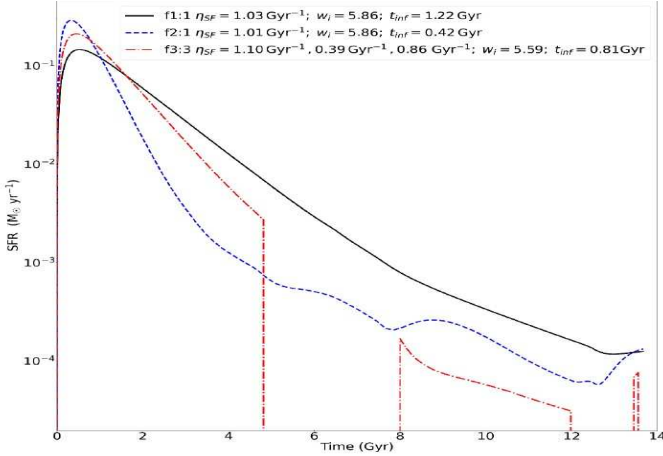


FIGURE 1. Star formation rate (SFR) as a function of time for three distinct models, represented by different colors and line styles. The solid black line corresponds to a single episode of star formation with $\eta_{\text{SF}} = 1.01 \text{ Gyr}^{-1}$, $w_i = 5.86$, and $t_{\text{inf}} = 1.22 \text{ Gyr}$. The dashed blue line represents another single-episode model with $\eta_{\text{SF}} = 1.01 \text{ Gyr}^{-1}$, $w_i = 5.86$, and $t_{\text{inf}} = 0.42 \text{ Gyr}$. The red dash-dot line depicts a scenario with three distinct star formation episodes, with efficiencies of $\eta_{\text{SF}} = 1.10 \text{ Gyr}^{-1}$, 0.39 Gyr^{-1} , and 0.86 Gyr^{-1} , $w_i = 5.59$, and $t_{\text{inf}} = 0.81 \text{ Gyr}$.

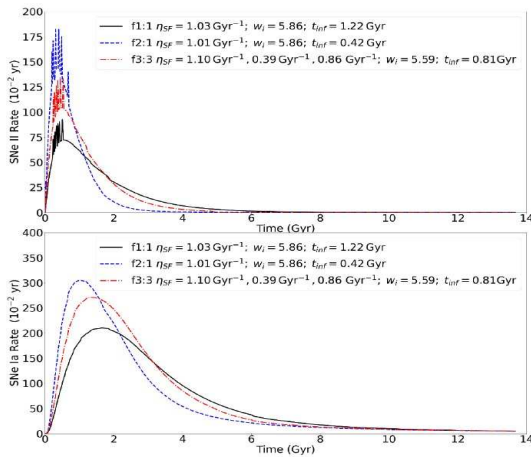


FIGURE 2. The top panel shows the Type II supernova (SNe II) rate as a function of time, while the bottom panel shows the Type Ia supernova (SNe Ia) rate as a function of time. The different lines represent the same parameters used in Fig. 1.

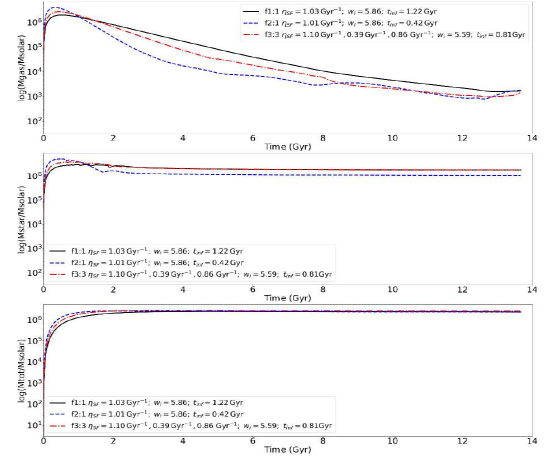


FIGURE 3. Upper panel: gas mass as a function of time. Middle panel: stellar mass as a function of time. Lower panel: total mass as a function of time.

5. Conclusions

This study examined the chemical evolution of the Fornax dwarf spheroidal galaxy using models calibrated with observational data, testing three scenarios with different star formation efficiencies (η_{SF}), infall timescales (t_{inf}), and wind efficiencies. Model 1 ($\eta_{\text{SF}} = 1.03 \text{ Gyr}^{-1}$, $w_i = 5.86$, $t_{\text{inf}} = 1.22 \text{ Gyr}$) provided the best match to the stellar metallicity distribution, reproducing the fraction of stars with $[\text{Fe}/\text{H}] \approx -1.0$ dex. In this model, SNe II peak at 0.31 Gyr and SNe Ia at 1.8 Gyr, indicating gradual enrichment. Final masses are $2.37 \times 10^6 M_{\odot}$ (total), $1.79 \times 10^6 M_{\odot}$ (stars), and $1.69 \times 10^3 M_{\odot}$ (gas), showing that most gas was consumed or lost. Model 1 therefore best represents Fornax's chemical evolution, reproducing MDF and abundance trends while indicating star formation episodes and gas loss. These results provide supernova rates and mass estimates to guide future 3D hydrodynamical simulations and enhance understanding of winds, star formation, and metallicity in Fornax.

References

- Battaglia, G. et al. 2006, *A&A*, 459, 423
 Caproni, A. et al. 2015, *ApJ*, 805, 109
 Caproni, A. et al. 2017, *ApJ*, 851, L39
 Coleman, M. & de Jong, J. T. A. 2008, *ApJ*, 685, 933
 de Boer, T. J. L. et al. 2012a, *A&A*, 539, A103
 de Boer, T. J. L. et al. 2012b, *A&A*, 544, A73
 Dolphin, A. E. et al. 2005, *MNRAS*, 357, 25
 Fenner, Y. et al. 2006, *ApJ*, 646, 184
 Geisler, D. et al. 2005, *AJ*, 129, 1428
 Hendricks, B. et al. 2014, *ApJ*, 785, 102
 Hill, V., Tolstoy, E. & Tosi, M. 2009, *ARA&A*, 47, 371
 Ikuta, C. & Arimoto, N. 2002, *A&A*, 391, 55
 Kirby, E. N. et al. 2010, *ApJS*, 191, 352
 Koch, A. et al. 2013, *ApJ*, 775, 58
 Kunth, D. & Östlin, G. 2000, *A&ARv*, 10, 1
 Lanfranchi, G. A. & Matteucci, F. 2003, *MNRAS*, 345, 71
 Lanfranchi, G. A. & Matteucci, F. 2004, *MNRAS*, 351, 1338
 Lanfranchi, G. A. & Matteucci, F. 2010, *A&A*, 512, A85
 Letarte, B. et al. 2006, *A&A*, 453, 547
 Letarte, B. et al. 2010, *A&A*, 523, A17
 Mateo, M. 1998, *ARA&A*, 36, 435
 Pont, F. et al. 2004, *MNRAS*, 350, 1385
 Ruiz, L. O. et al. 2013, *ApJ*, 767, 146
 Shetrone, M. et al. 2001, *AJ*, 122, 2099
 Shetrone, M. et al. 2003, *AJ*, 125, 684
 Tolstoy, E., Hill, V. & Tosi, M. 2009, *ARA&A*, 47, 371
 Venn, K. A. et al. 2004, *AJ*, 128, 1177
 Venn, K. A. et al. 2012, *ApJ*, 751, 102
 Walker, M. G. et al. 2007, *ApJS*, 171, 389